Cancer Biology and Translational Studies

Molecular Cancer Therapeutics

Analysis of the Genomic Landscape in ALK+ NSCLC Patients Identifies Novel Aberrations Associated with Clinical Outcomes

Mathilde Couëtoux du Tertre[1,2], Maud Marques[1,2], Lise Tremblay[3], Nicole Bouchard[4], Razvan Diaconescu[5], Normand Blais[6], Christian Couture[3], Vincent Pelsser[1], Hangjun Wang[1], Valerie Higenell[2], Luisa Izzi[2], Karen Gambaro[1,2], Cyrla Hoffert[1,2], Archana Srivastava[1,2], Alan Spatz[1], Caroline Rousseau[1], Suzan McNamara[1,2], Victor Cohen[1], Gerald Batist[1], and Jason Agulnik[1]

Abstract

Rearrangements in the anaplastic lymphoma kinase (*ALK*) gene are found in approximately 5% of non–small cell lung carcinoma (NSCLC). Here, we present a comprehensive genomic landscape of 11 patients with ALK+ NSCLC and investigate its relationship with response to crizotinib. Using whole-exome sequencing and RNAseq data, we identified four rare ALK fusion partners (*HIP1*, *GCC2*, *ERC1*, and *SLC16A7*) and one novel partner (*CEP55*). At the mutation level, *TP53* was the most frequently mutated gene and was only observed in patients with the shortest progression-free survival (PFS). Of note, only 4% of the genes carrying mutations are present in more than 1 patient. Analysis of somatic copy number aberrations (SCNA) demonstrated that a gain in EML4 was associated with longer PFS, and a loss of *ALK* or gain in *EGFR* was associated with shorter PFS. This study is the first to report a comprehensive view of the ALK+ NSCLC copy number landscape and to identify SCNA regions associated with clinical outcome. Our data show the presence of *TP53* mutation as a strong prognostic indication of poor clinical response in ALK+ NSCLC. Furthermore, new and rare ALK fusion partners were observed in this cohort, expanding our knowledge in ALK+ NSCLC.

Introduction

Lung cancer is the leading cause of cancer-related death worldwide with 85% of the cases being non–small cell lung cancer (NSCLC). Major advances in NSCLC have led to the identification of at least one oncogenic driver mutation in 64% of patients (1, 2). Development of targeted therapies against some of these genomic abnormalities has brought treatment of lung cancer into the era of precision medicine. Rearrangements in the anaplastic lymphoma kinase (*ALK*) gene were identified as an oncogenic driver event in 2007, and are found in 3%–7% of NSCLC, typically in younger patients who are light- or nonsmokers (3, 4). Echinoderm microtubule-associated protein-like 4 (*EML4*) is the main fusion partner of *ALK* representing about 80% of the ALK+ cases, and more than a dozen different *EML4-ALK* variants have been identified (5).

Clinical management of patients with ALK+ NSCLC has been revolutionized by the development of therapies that specifically inhibit ALK kinase activity. Crizotinib, an orally available ATP-competitive small molecule, was the first ALK tyrosine kinase inhibitor (ALK-TKI) used in the clinical setting. However, most patients relapse within 1–2 years (6) due to the generation of on-target resistance (through acquisition of secondary mutations in the tyrosine kinase domain of ALK) and/or off-target resistance (through activation of alternative signalling pathways; ref. 7). Second- and third-generation ALK inhibitors have been developed to address some of the resistance mechanisms to crizotinib and have activity against a wide spectrum of secondary ALK mutations, as well as increased potency, selectivity, and blood–brain barrier permeability (8–12). However, acquired resistance to next-generation ALK-TKIs is also observed and is harder to overcome with the appearance of compound mutations in ALK as well as loss of ALK dependency by activation of alternative pathways. Despite tremendous effort and investment in drug development, the acquisition of resistance remains a major challenge across ALK-TKIs, for which there are currently no predictive biomarkers.

Decreasing costs of next-generation sequencing (NGS) technologies have enabled researchers and clinicians to further investigate the mutational and copy number aberration landscape of lung cancer using whole-genome or whole-exome sequencing

[1]Segal Cancer Centre, Jewish General Hospital, McGill University, Montreal, Quebec, Canada. [2]Exactis Innovation, Montreal, Quebec, Canada. [3]Institut Universitaire de Cardiologie et Pneumologie de Quebec, Universite de Laval, Quebec City, Quebec, Canada. [4]Centre Hospitalier Universitaire de Sherbrooke, Sherbrooke, Quebec, Canada. [5]Hopital Sacre Cœur Montreal, Montreal, Quebec, Canada. [6]Centre Hospitalier Universitaire de Montreal, Montreal, Quebec, Canada.

Note: Supplementary data for this article are available at Molecular Cancer Therapeutics Online (http://mct.aacrjournals.org/).

M. Couëtoux du Tertre and M. Marques contributed equally to this article.

Corresponding Authors: Gerald Batist, Segal Cancer Centre, Sir Mortimer B. Davis Jewish General Hospital, 3755 Cote-Ste-Catherine Road, Montreal, Quebec H3T 1E2, Canada. Phone: 514-340-8222; Fax: 514-340-8708; E-mail: gerald.batist@mcgill.ca; and Jason Agulnik, jagulnik@jgh.mcgill.ca

Mol Cancer Ther 2019;18:1628–36

doi: 10.1158/1535-7163.MCT-19-0105

(WES). Several genomic studies provided a list of key genes affected in lung adenocarcinoma such as *TP53*, as well as actionable genes like *EGFR*, *KRAS*, *ERBB2*, and *PIK3CA*. However, the lower occurrence of ALK rearrangements in the population made this cohort difficult to study and comprehensive genomic studies of ALK+ NSCLC are limited and are mostly lacking clinical outcomes.

In this study, we analyzed WES from pretreatment primary and posttreatment metastatic tumors of 11 patients with ALK+ NSCLC treated with crizotinib as standard of care. We identified rare ALK fusion partners, as well as somatic mutation and copy number aberrations associated with response to crizotinib.

Materials and Methods

Study oversight

We conducted a prospective observational study (NTC-02041468) at five major cancer centers in Canada. The study was approved by the institutional review board at each participating hospital and complied with Good Clinical Practices, the principles of the Declaration of Helsinki, and all applicable regulatory requirements. All patients provided written informed consent prior to any study specific procedures.

Trial design, treatment, and assessments

This study was performed in a real-life context for patients with locally advanced or metastatic ALK+ NSCLC between January 31, 2014 and July 31, 2018 (cut-off date). Objectives included confirmation of measures of efficacy of crizotinib therapy [progression-free survival (PFS), disease control rate, and time to treatment discontinuation) and assessment of blood- and tissue-based biomarkers of response or resistance to crizotinib. Eligible patients had histologic confirmation of ALK+ NSCLC. Radiologic disease assessment was performed within 30 days of starting treatment and every 8–12 weeks during treatment until progression. Measurable disease was assessed according to the RECIST v.1.1 (13).

Patients received oral crizotinib as capsules at a dose of 250 mg twice daily, or 200 mg twice daily in the case of toxicity. Treatment with crizotinib followed standard of care and continuation beyond progression of disease was at the discretion of the treating physician. At the cut-off date, 6 (25%) patients had a partial response, 9 (37.5%) had stable disease, 5 had progressive disease, and response data was not available for 4 patients (Supplementary Table S1). An objective response rate of 25% and a durable clinical response of 62.5% were achieved, and 2 patients (8.3%) were still responding to treatment at the cut-off date (Supplementary Table S1). Five of 24 patients (20.8%) were already receiving crizotinib therapy when enrolled in this study. Two of these 5 patients were treated with crizotinib in combination with the HSP90 inhibitor onalespib (AT13387; Astex Pharmaceuticals) in a previous clinical trial (NCT01712217).

Tissue and blood sample collection

The pretreatment tissues were archived, formalin-fixed, paraffin-embedded (FFPE) from primary lung tumor collected at diagnosis by ultrasound-guided needle core biopsy, fine-needle aspiration, or endobronchial ultrasound transbronchial needle aspiration. We obtained primary FFPE samples for 21 of 24 patients (87.5%). Five of these patients (20.8%) underwent a posttreatment biopsy at disease progression. Posttreatment biopsies were obtained from a metastatic hepatic lesion (3 patients), a progressing lung lesion (1 patient), or the right hilar lymph node (1 patient). Samples were either snap frozen in liquid nitrogen and embedded in optimal cutting compound temperature or FFPE. Hematoxylin and eosin staining was performed on 4–5-μm sections, which were then submitted for histopathologic review by a designated pathologist. ALK rearrangement status was assessed on FFPE primary lung tumor or fine-needle aspirates either by IHC using ALK antibody clones 5A4 (Novocastra or Biocare) or D5F3 (Cell Signaling Technology), or by FISH using the FISH Vysis LSI ALK Break Apart FISH Probe Kit.

Tissues passed histologic quality control if the viable neoplastic cell content was over 40% and were subsequently processed for nucleic acid extraction.

DNA and RNA isolation

Coextraction of DNA and RNA from FFPE and frozen samples was performed with the AllPrep DNA/RNA FFPE Kit and the All Prep DNA/RNA Mini Kit, respectively (Qiagen). The QIAamp DNA FFPE Kit (Qiagen) was used for isolation of FFPE DNA alone. DNA was extracted from buffy coat using the Gentra PureGene Blood Kit (Qiagen). All extractions were performed according to the manufacturer's instructions. The NanoDrop Spectrophotometer (Thermo Fisher Scientific), Qubit v2.0 Fluorometer (Thermo Fisher Scientific), and the Agilent Bioanalyzer 2100 (Agilent Technologies) were used to assess concentration, purity, and degradation of nucleic acid extracts. Samples with RIN > 3 were used for total RNA sequencing. RNA was extracted only from 3 patients and DNA from 11 patients.

Whole-exome library preparation, sequencing, and data analysis

WES was performed on 50 ng of DNA isolated from all tumor tissue samples that passed quality control and yielded sufficient material. Target enrichment was carried out using the Agilent SureSelect Human Exome XT HS v6 Kit (Agilent Technologies) according to the manufacturer's protocol. Custom baits were designed in the *ALK* gene and known ALK fusion partner introns (Supplementary Table S2). Sequencing was performed on Illumina HiSeq2500 with 125 base pair (bp) paired-end reads. An average of 90 M reads per sample was obtained. Data can be found under the following SRA accession number PRJNA514317.

Raw sequences were preprocessed with Trimmomatic to remove adaptor contamination, low quality bases, and shorter reads. Clean reads were aligned to the reference genome (UCSC hg19) using the Burrows-Wheeler Aligner maximal exact matches algorithm. The Genome Analysis Toolkit software was used to mark duplicates and do realignments around Indels.

Somatic variants were identified using MuTect2 with matched tumor and normal samples. Variants were annotated with ANNOVAR (applied filters: MuTect2 filter = "PASS", number of reads = 10, number of alternative reads = 5, minimum alternative allelic frequency for SNP = 5%, and minimum alternative frequency for Indel = 10%). Sequenza was used to assign cellularity and variant allelic fraction (VAF) was normalized according to each sample cellularity (14).

FACTERA was used to detect fusions between the genomic region encompassing introns 18 and 19 of the *ALK* gene and the genomic regions covered by custom baits. Default settings were used except for the parameter for number of read overlapping the fusion (option -r) that was set at 2 (15).

Somatic copy number analysis

Nexus Biodiscovery v9 (BioDiscovery Inc.) was used to analyze somatic copy number aberrations (SCNA) from WES data following the removal of read duplicates. Copy number was estimated by comparing the primary or metastatic tumor lesions with the matched normal sample. The ngCGH (matched) processing setting was used for our analysis. The frequency plot was obtained using the view, aggregate, and copy number parameters. Significant regions were obtained using the STAC algorithm. The Nexus predictive survival tool was used to identify regions associated with PFS. Regions for which less than 3 patients/group had gains or losses were not included.

ALK fusion validation

To validate ALK fusion in our patient samples, we designed primers to encompass the breakpoint identified by FACTERA.

RNA library preparation, sequencing, and data analysis

Ribosomal depletion and RNA libraries were performed with Ribo-Zero (Illumina) and the TruSeq Adaptor Kit (Illumina). Libraries were sequenced as 125 bp paired-end reads on Illumina HiSeq 2500 (Genome Quebec). Raw FASTQ sequences were trimmed and filtered with Trimmomatic v0.3228. Trimmed reads were aligned to the reference genome (UCSC hg19) using STAR v2.3.0e. Quality control was performed using metrics obtained with FASTQC v0.11.2, SAMtools, and BEDtools. FeatureCount was used for counting RNA-seq reads at the gene level. Fusions were detected manually and using STAR-Fusion.

Results

Sample collection, patient characteristics, and clinical outcome

Twenty-four locally advanced or metastatic patients with ALK+ NSCLC were enrolled in this study and administered at least one dose of crizotinib. The objective was to recover DNA and, when feasible, RNA from primary lesions prior to treatment and metastatic lesions posttreatment collected at progression to identify potential biomarkers of response or resistance to crizotinib (Fig. 1). For 3 patients (12.5%), primary samples were not available and for the remaining 21 patients, 42.9% of the samples failed histology quality control (HQC). Most of the samples passing HQC (83.3%) yielded enough DNA to be used for NGS.

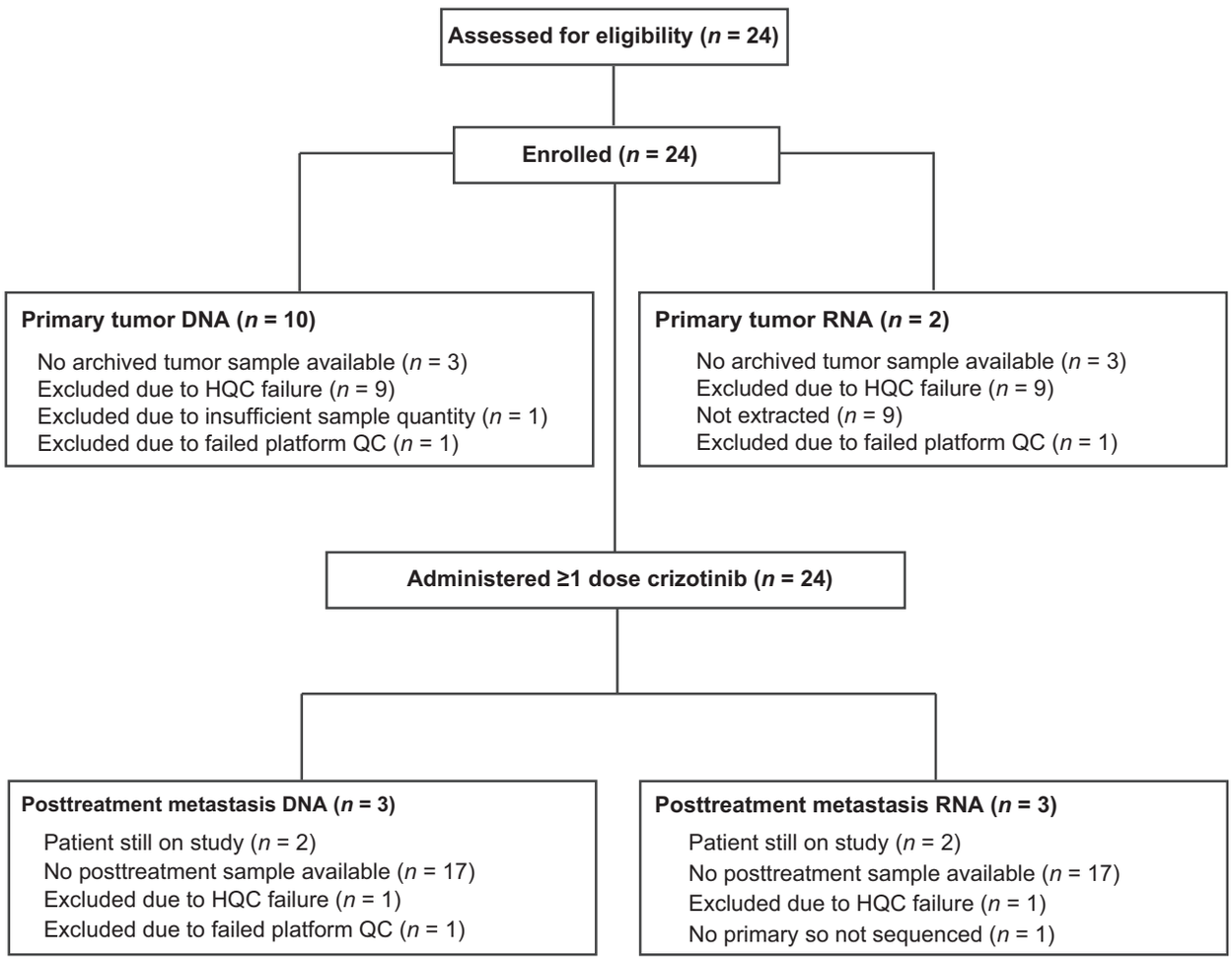

Figure 1.
Patient samples' profiling flowchart. Overview of the samples collected and processed during the study.

These numbers highlight the difficulty to obtain high quality specimens from patients with lung cancer. For 19 patients (79.2%) no second biopsies were collected, including 2 patients that did not progress at date of data cutoff (Fig. 1). Overall, 10 pretreatment primary lesions and 3 posttreatment metastatic lesions collected from 11 patients passed quality control criteria and were analyzed by WES (Fig. 1). RNA was extracted from six samples from 3 patients, and only five passed QC and were sequenced (Fig. 1). Despite the small number of patients in this study due the rarity of this patient subset, coupled with the challenges of obtaining adequate samples, often observed in lung cancer, this report deepens our understanding of genomic mechanisms that may enable advances in ALK+ NSCLC treatment.

Table 1 summarizes the demographic, clinical, and baseline characteristics of the entire cohort, as well as the patients profiled. We observed a median PFS of 13.1 months (range, 1.1–43.6 months; 95% confidence interval, 4–26.9 months). The association between some of these characteristics and PFS in response to crizotinib was assessed using a multivariate Cox proportional hazard ratio on the entire cohort (Supplementary Fig. S1). Although we did not observe any significant associations between the demographics, baseline, or clinical characteristics tested, and response duration, we did observe that smokers and patients with an Eastern Cooperative Oncology Group (ECOG) of 1 tended to have a shorter PFS.

Table 1. Demographic, clinical, and baseline patient characteristics

	Genomic cohort ($n = 12$)	Entire cohort ($n = 24$)
Age (years)		
Median	62.5	62
Min–max	41–78	41–80
Sex		
Male	8 (66.7%)	14 (58.3%)
Female	4 (33.3%)	10 (41.6%)
Weight (kg)		
Median	77.7	77.5
Min–max	40–104	40–127.6
Ethnicity		
White or Caucasian	10 (83.3%)	20 (83.3%)
African-American	1 (8.3%)	2 (8.3%)
Hispanic	1 (8.3%)	2 (8.3%)
ECOG performance status		
0	4 (33.3%)	10 (41.6%)
1	7 (58.3%)	12 (50%)
Unknown	1 (8.3%)	2 (8.3%)
Smoker[a,b]		
Yes	2 (16.7%)	4 (16.7%)
No	10 (83.3%)	20 (83.3%)
Histology		
Adenocarcinoma	11 (91.7%)	23 (95.8%)
Mixed	1 (8.3%)	1 (4.2%)
Stage at initial diagnosis		
III	0	1 (4.2%)
IIIa	1 (8.3%)	1 (4.2%)
IIIb	1 (8.3%)	3 (12.5%)
IV	10 (83.3%)	19 (79.2%)
EGFR mutation		
Negative	12 (100%)	24 (100%)
Positive	0	0
Line of treatment		
First-line	9 (75%)	21 (87.5%)
Second-line	3 (25%)	3 (12.5%)
Number of previous anticancer therapies		
0	9 (75%)	18 (75%)
1	3 (25%)	6 (25%)
Number of distant metastatic sites at study baseline		
0	3 (25%)	4 (16.65%)
1	3 (25%)	10 (41.7%)
2	2 (16.7%)	6 (25%)
≥3	4 (33.3%)	4 (16.65%)

[a]Smokers are defined as subjects that smoked at the time of enrollment or stopped within 12 months of enrollment.
[b]Nonsmokers are defined as subjects that smoked ≤5 packs/year and stopped smoking at least 12 months prior to enrollment.

Identification of ALK rearrangements using RNAseq and targeted sequencing

Because of the challenges faced in the dual collection of DNA and RNA in the first 3 patients processed, we decided to focus on extracting only DNA for the remaining samples. To identify ALK rearrangement from DNA, we designed custom probes covering ALK intron 18 and intron 19, as well as introns for some of well-known ALK fusion partners (Supplementary Table S2) and included them in the SureSelect V6 probes used for WES. We identified *ALK* rearrangements in 12 patients using WES and/or RNA sequencing data (Table 2). In patients with both RNAseq and WES available, the same *ALK* rearrangement was identified with both methods (Supplementary Fig. S2A and S2B). We found that 8 of 12 patients (66%) had an *EML4-ALK* fusion, with variants 1, 3, and 5 being expressed in 2 (16.7%), 5 (63%), and 1 (8.3%) patients, respectively (Table 2). Previous publications reported that expression of variant three was associated with poor response to crizotinib (16). Accordingly, we observed that 4 of the 5 patients expressing variant three rapidly progressed. However, the remaining patient expressing variant three had a PFS of 29.5 months, highlighting that specific *ALK* variant expression alone is not sufficient to explain differences in response duration. Despite the relatively small size of our cohort we identified four rare *ALK* fusions partners, *ERC1*, *SLC16A7*, *HIP1*, and *GCC2* and one novel, *CEP55*. *ERC1* is known to be a fusion partner with tyrosine kinase proteins *RET* and *ROS1* (17–22). Interestingly, all the patients carrying these unusual *ALK* fusion partners had a longer PFS (range: 22.4–40.7 months; Table 2).

Mutational landscape of ALK+ pretreatment primary and posttreatment metastatic tumors

Mutation profiles across patients with ALK+ NSCLC were found to be highly heterogeneous. The tumor mutation burden ranges from 0.23 to 4.86 mutation/Mb of exon (Fig. 2A). No clear relationship with patient smoking status was observed. The number of mutations and chromosomal rearrangements is not inversely correlated in this cohort (Fig. 2A) and the number of each type of events by patient is summarized in Supplementary Table S3. Consistent with data reported on lung adenocarcinoma, *TP53* was the most frequently mutated gene identified in our cohort in 3 of 11 patients (27%), along with two other genes *FBN2* and *FRMD4A*. Focusing on previously reported genes affected in NSCLC (3), Fig. 2B shows the frequency of mutation and copy number aberrations for the following genes *TP53*, *EGFR*, *STK11*, *CDKN2A*, *PTEN*, *RB1*, *MET*, *ERBB2*, and *BRAF*. Most of the genes targeted by a mutation were unique for each patient (Fig. 2C), with only 4% identified in more than one patient. As previously reported, *TP53* mutation was associated with poor PFS (Fig. 2D), interestingly the loss of *TP53* did not associate with a worse outcome (Fig. 2E), which may indicate a functional

Table 2. List of ALK rearrangements in primary tumor[a] and posttreatment lesion[b]

Patient ID	PFS (months)	Time	Technology	ALK Exon	Partner (exon, variant)	Supporting reads	ALK mutation
003	4	Post	RNAseq	E20	EML4 (E6, V3)	NA	
004	1.6	Pre	WES, RNAseq	E20	EML4 (E6, V3)	14/105	
		Post	WES, RNAseq	E20	EML4 (E6, V3)	30/169	
007	4.5	Pre	WES	E20	EML4 (E13, V1)	31/190	
011	1.6	Pre	WES, RNAseq	E20	EML4 (E6, V3)	104/450	
		Post	WES, RNAseq	E20	EML4 (E6, V3)	56/518	
013	26.9	Post	WES	E20	HIP1 (E28)	78/440	G1202R
015	22.4	Pre	WES	E20	GCC2 (E18)	3	
016	29.5	Pre	WES	E20	EML4 (E6, V3)	20/369	
017	14	Pre	WES	E20	EML4 (E13, V1)	15/401	
018	18.7	Pre	WES	E20	EML4 (E18, V5)	33/200	
021	0.98[c]	Pre	WES	E20	CEP55 (E3)	3	
022	1.5	Pre	WES	E20	EML4 (E6, V3)	12/422	
025	40.7[d]	Pre	WES	E20	ERC1 (E15)	5/57	
					SLC16A7(E1)	4/53	

[a]Identified as pre in time column.
[b]Identified as post in time column.
[c]Patient discontinued because of drug toxicity.
[d]Patient currently on study.

difference between the loss and mutated *TP53* in tumor biology (23).

No mutations in *ALK* were found in primary lesions, even in patients exhibiting intrinsic resistance to crizotinib, again pointing to alternative mechanisms of resistance. In a posttreatment lesion from a patient with acquired resistance, we detected a known mutation in *ALK* (G1202R) associated with crizotinib and ceritinib resistance (Table 2; ref. 24). Absence of *ALK* mutations in primary tumors as well as posttreatment metastatic tumors in intrinsically resistant patients emphasizes the need to understand off-target resistance mechanisms in patients with ALK+ NSCLC.

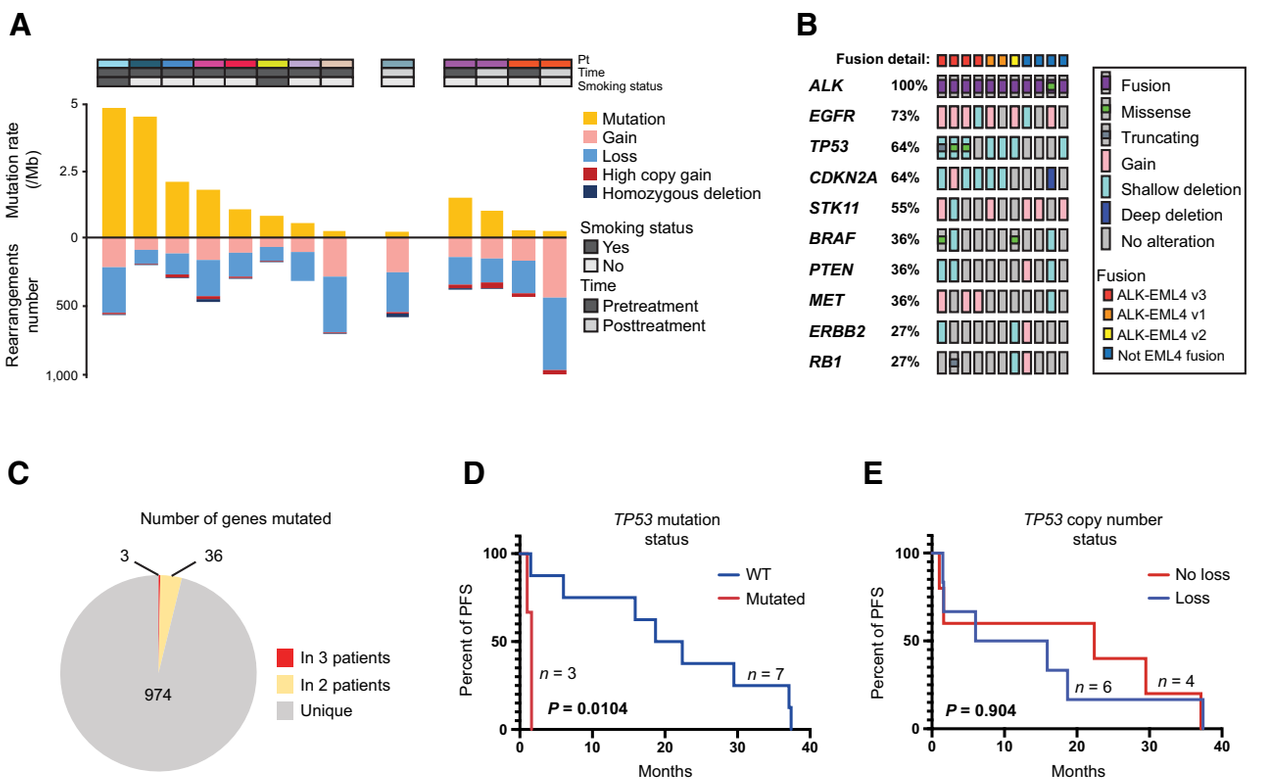

Figure 2.
Mutational landscape of patients with ALK+ NSCLC. **A,** Number of mutation and copy number aberrations per sample. Patients are grouped as follows: prelesion only ($n = 8$), postlesion only ($n = 1$), and pre- and postlesions ($n = 2$). **B,** Oncoplot of genomic alteration occurring in genes known to be affected in lung adenocarcinoma. **C,** Pie chart showing the number of genes mutated in 3 patients, 2 patients, or 1 patient. Kaplan–Meier curves associating the PFS with *TP53* mutation (**D**) or deletion (**E**).

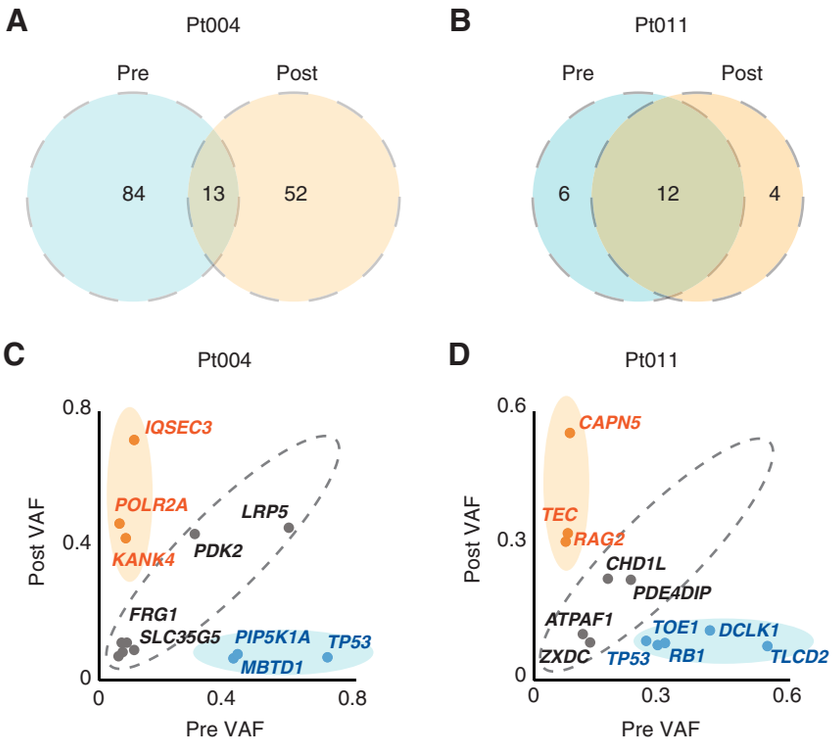

Figure 3.
Heterogeneity in patients with paired samples. Venn diagram showing the number of genes mutated in primary, metastasis, or both for patient 004 (**A**) and patient 011 (**B**). Scatter plot showing the VAF for each common mutation between primary and metastatic lesion for patient 004 (**C**) and patient 011 (**D**). In gray are the mutations with similar VAF between primary and metastasis. In blue, mutations with VAF higher in the primary lesion. In orange, mutations with VAF higher in the metastatic lesion.

Mutational heterogeneity in patients with pre- and postbiopsies

Data from prior and post crizotinib treatment biopsies were obtained for 2 intrinsically resistant patients (patient #004 and #011). To take advantage of these paired biopsies from 2 patients with similar response, we decided to perform a deeper analysis of intrapatient heterogeneity. Of note, despite both patients having no response to crizotinib, the total number of mutations in each patient is very different (97 vs. 18, in the primary lesion; Fig. 3A). Interestingly, the number of common mutations between pre- and posttreatment biopsies were similar between both patients (12 and 13). These common mutations represented approximately 66.7% of the primary lesion for patient 011, but only represented approximately 13.4% of the primary lesion for patient 004 (Fig. 3A).

Next, we looked at the VAF of the common mutations between both lesions for each patient. We distinguished three types of mutations: one that had consistent VAF between both lesions (grey), one that had higher VAF in the pretreatment lesion (blue), and one which had higher VAF in the posttreatment lesion (orange; Fig. 3C and D). Interestingly, in both patients *TP53* VAF was lower in the postmetastatic lesion compared with the primary lesion, which could be attributed to treatment or the difference in lesion localization (primary vs. metastasis). *TP53* was the only gene mutated in both patients. In patient 004, we identified a mutation in *LRP5* (NM_001291902 p.D559V), a gene previously reported to mediate EGFR and c-Met TKIs, erlotinib, and SU11274 resistance (25).

SCNA in patients with ALK+ NSCLC

We then assessed the SCNA landscape in ALK+ primary tumors from 10 patients. Given the absence of published SCNA data in patients with ALK+ NSCLC, we compared our cohort with the Cancer Genome Atlas (TCGA) data for lung adenocarcinoma, which includes ALK− and potentially some ALK+ patients (3). We observed a similar SCNA profile compared with TCGA data with the main gains occurring on chr1q, chr5p, chr7p and major losses on chr17p and chr18q (Fig. 4A and B). Despite the small size of our cohort, we also identified several differences between our ALK+ samples and lung adenocarcinoma, including losses occurring in chr2p (specifically at the *ALK* locus), and gains in chr5q. We next used the Nexus Copy Number predictive survival power tool to identify regions associated with crizotinib-related PFS. Overall, 190 regions were significantly associated with PFS (permutated $P < 0.1$), including 120 losses and 70 gains (Supplementary Table S4). Notably, three of these regions contained genes associated with ALK+ NSCLC, including *ALK* itself and two known fusion partners *KIF5B* and *EML4*. While loss of *ALK* is associated with shorter PFS (Fig. 4C), we observed that a gain of *EML4* is associated with a longer PFS (Fig. 4D). Despite the absence of *EGFR* somatic mutations in our cohort, a known mechanism of resistance to crizotinib, we observed an association between the amplification of the *EGFR* locus and a shorter PFS (Fig. 4E). Interestingly, only the poor responder group (3/3) had a cooccurrence of *ALK* loss and *EGFR* amplification. These observations will be interesting to further assess in a larger cohort.

Surprisingly, considering the size of our cohort, three amplified regions (chr4:41,496,634–41,511,536; chr4:186,272,784–186,295,411; and chr4:183,549,846–184,616,629) showed high significance in predicting better PFS. Using RNAseq data from TCGA lung adenocarcinoma publicly available on the human protein atlas (www.proteinatlas.org), we observed that higher expression of certain genes contained in these intervals

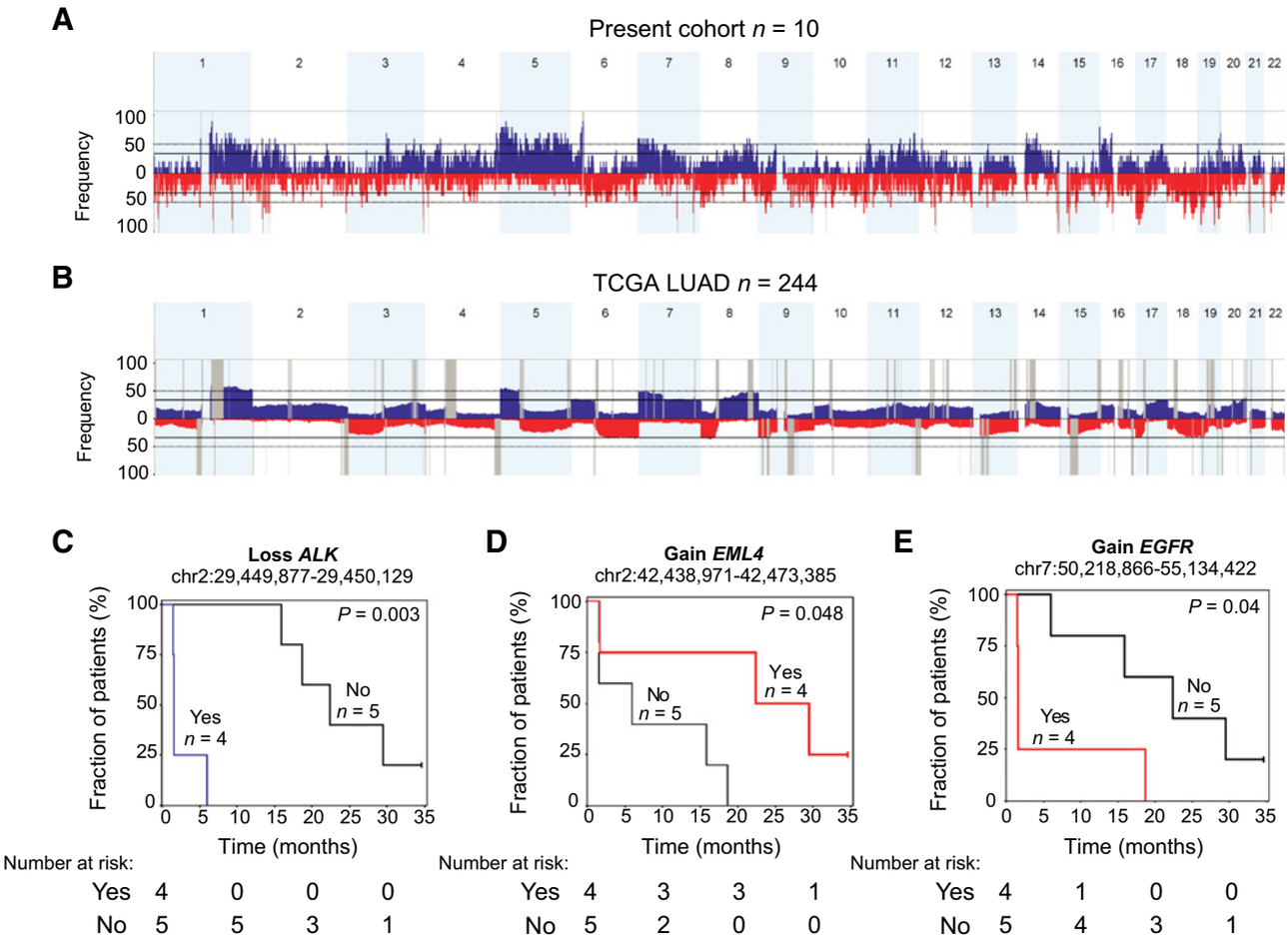

Figure 4.

SCNA profile shows specific ALK+ NSCLC structural variants associated with PFS. **A,** SCNA profile from this cohort ($n = 10$); significant regions are in gray. **B,** SCNA profile from TCGA lung adenocarcinoma data (Nexus TCGA premier, $n = 244$); significant regions are in gray. Three examples of regions significantly associated with PFS: *ALK* (**C**), *EML4* (**D**), and *EGFR* (**E**).

(*SNX25*, *LRP2BP*, and *LIMCH1*) is also significantly associated with longer overall survival.

Discussion

To date, the mutational and copy number landscapes of ALK+ NSCLC tumors have not been well characterized. In this study, we identified rare ALK fusion partners: *ERC1*, *SLC16A7*, *HIP1*, and *GCC2*, as well as copy number aberrations associated with PFS.

The first challenge in profiling studies occurs during sample collection. Good quality biopsies are difficult to obtain from patients with lung cancer, and in this study 50% of the samples failed at the HQC step (low cellularity) and consequently were not used for further analysis. As a vast proportion of ALK-TKI inhibitor resistance is mediated by off-target effects (7, 8), we believe that future studies should include genomic and transcriptomic data to fully uncover these mechanisms. Despite being able to identify a mutation (*TP53*) and copy number aberrations associated with response to crizotinib, our limited number of RNA samples impaired our capacity to interrogate similar changes in gene expression of specific pathways, which may have unveiled novel mechanisms of resistance to crizotinib in the absence of ALK mutations.

In cancer, intrinsic and acquired resistances are often driven by different mechanisms. In one case, a total absence of response is noted and in theory no selection pressure has been applied on the tumor. On the other hand, acquired resistance mechanisms appear following a period of response to a specific intervention and are the result of emergence of new mutations, genomic events, or changes in gene expression favoring tumor growth. Intrinsic and acquired resistance mechanisms are highly heterogeneous. In the case of crizotinib, several studies reported mechanisms of acquired resistance mainly involving mutations in the *ALK* gene (26). In this study, we were able to obtain only one postbiopsy from a patient with acquired resistance and an ALK-G1220R mutation was detected which is known to induce crizotinib resistance. Recent studies showed a clear association between *TP53* mutation and worse PFS (23, 27), and we were able to observe a similar effect in our cohort with 3 of 3 intrinsically

resistant patients having *TP53* mutated, yet *TP53* mutation alone was not sufficient because 1 patient carrying *TP53* mutation was not resistant. All the missense mutations (NM_001276760: R117P, R136L, and R243W) identified are targeting arginine residues located in the DNA binding site of p53, potentially affecting the electrostatic charge of the domain (28). Further studies on the impact of these mutations on p53 binding as well as its transcriptional network will bring valuable information on p53 biology.

Modification of VAF during course of treatment or disease progression is challenging to track considering numerous confounding factors such as cellularity and copy number estimate. However, understanding these changes can give valuable information on drug resistance mechanisms as well as metastatic dissemination. In this cohort, we observed for the first time a lower VAF for *TP53* mutation in metastatic posttreatment lesions compared with primary tumor in 2 of 2 intrinsically resistant patients. It will be interesting to determine the factors influencing this change in an independent cohort.

This study reports for the first time the copy number landscape of patients with ALK+ NSCLC showing similarities with the lung adenocarcinoma copy number landscape with amplification of chr1q, chr5p, and chr7p and chr7q (3). Because our cohort had detailed clinical parameters, we were able to identify significant association between genomic aberrations and PFS. To our knowledge, this study is also the first to report predictive chromosomal anomalies which warrant further validation in independent crizotinib studies. Furthermore, given the similarity of mechanism of action among ALK-TKIs, these identified aberrations associated with response may also apply to next-generation ALK-TKIs.

Our findings provide valuable data on rare and novel ALK fusions and genomic aberrations potentially involved in ALK+ NSCLC PFS and resistance to crizotinib. In contrast to previously published work (29, 30), specific EML4-ALK variants were not sufficient to explain patient response to crizotinib in our cohort. In addition, the article highlights novel concurrent genomic events (loss of *ALK* and gain of *EGFR*) only present in intrinsically resistant patients and confirmed unfavorable association between ALK rearrangement and *TP53* mutation for patient outcome (23, 27). Because of the small sample size in our study, further validation will be essential to confirm our observations in crizotinib or other ALK-TKI–treated patients with ALK+ NSCLC. Priority should be given to further confirm and validate TP53 mutation as a poor prognostic indicator in patients treated with ALK-TKIs.

Disclosure of Potential Conflicts of Interest

N. Bouchard has received speakers bureau honoraria from Pfizer. C. Couture has received speakers bureau honoraria from and is a consultant/advisory board member for Pfizer. A. Spatz is a consultant/advisory board member for Pfizer. No potential conflicts of interest were disclosed by the other authors.

Authors' Contributions

Conception and design: M. Marques, C. Rousseau, S. McNamara, V. Cohen, G. Batist, J. Agulnik

Development of methodology: M. Couëtoux du Tertre, M. Marques, N. Blais, K. Gambaro, A. Spatz, C. Rousseau, S. McNamara

Acquisition of data (provided animals, acquired and managed patients, provided facilities, etc.): M. Marques, N. Bouchard, R. Diaconescu, N. Blais, C. Couture, V. Pelsser, H. Wang, K. Gambaro, C. Hoffert, A. Srivastava, A. Spatz, C. Rousseau, S. McNamara, V. Cohen, J. Agulnik

Analysis and interpretation of data (e.g., statistical analysis, biostatistics, computational analysis): M. Couëtoux du Tertre, M. Marques, N. Blais, V. Higenell, A. Spatz, S. McNamara, V. Cohen, G. Batist

Writing, review, and/or revision of the manuscript: M. Couëtoux du Tertre, M. Marques, L. Tremblay, R. Diaconescu, N. Blais, C. Couture, V. Higenell, K. Gambaro, C. Hoffert, C. Rousseau, S. McNamara, V. Cohen, G. Batist, J. Agulnik

Administrative, technical, or material support (i.e., reporting or organizing data, constructing databases): L. Izzi, K. Gambaro, C. Hoffert, A. Srivastava, C. Rousseau, S. McNamara

Study supervision: M. Couëtoux du Tertre, N. Blais, S. McNamara, G. Batist

Acknowledgments

The Q-CROC-05 study was funded by the Personalized Medicine Partnership for Cancer, the "Fonds de partenariat pour un Québec innovant et en santé (FPQIS)," and Pfizer. The study was initiated by Q-CROC and managed by Exactis Innovation, a Network of Centres of Excellence funded organization. We acknowledge the patients who enrolled in this study and made this project possible.

The costs of publication of this article were defrayed in part by the payment of page charges. This article must therefore be hereby marked *advertisement* in accordance with 18 U.S.C. Section 1734 solely to indicate this fact.

Received January 30, 2019; revised March 26, 2019; accepted June 19, 2019; published first June 26, 2019.

References

1. Kris MG, Johnson BE, Berry LD, Kwiatkowski DJ, Iafrate AJ, Wistuba II, et al. Using multiplexed assays of oncogenic drivers in lung cancers to select targeted drugs. JAMA 2014;311:1998–2006.
2. Travis WD, Brambilla E, Burke AP, Marx A, Nicholson AG. Introduction to the 2015 World Health Organization classification of tumors of the lung, pleura, thymus, and heart. J Thorac Oncol 2015;10:1240–2.
3. Cancer Genome Atlas Research Network. Comprehensive molecular profiling of lung adenocarcinoma. Nature 2014;511:543–50.
4. Soda M, Choi YL, Enomoto M, Takada S, Yamashita Y, Ishikawa S, et al. Identification of the transforming EML4-ALK fusion gene in non-small-cell lung cancer. Nature 2007;448:561–6.
5. Peters S, Taron M, Bubendorf L, Blackhall F, Stahel R. Treatment and detection of ALK-rearranged NSCLC. Lung Cancer 2013;81:145–54.
6. Solomon BJ, Mok T, Kim DW, Wu YL, Nakagawa K, Mekhail T, et al. First-line crizotinib versus chemotherapy in ALK-positive lung cancer. N Engl J Med 2014;371:2167–77.
7. Katayama R, Shaw AT, Khan TM, Mino-Kenudson M, Solomon BJ, Halmos B, et al. Mechanisms of acquired crizotinib resistance in ALK-rearranged lung Cancers. Sci Transl Med 2012;4:120ra17.
8. Gainor JF, Dardaei L, Yoda S, Friboulet L, Leshchiner I, Katayama R, et al. Molecular mechanisms of resistance to first- and second-generation ALK inhibitors in ALK-rearranged lung cancer. Cancer Discov 2016;6:1118–33.
9. Jain RK, Chen H. Spotlight on brigatinib and its potential in the treatment of patients with metastatic ALK-positive non-small cell lung cancer who are resistant or intolerant to crizotinib. Lung Cancer 2017;8:169–77.
10. Lin JJ, Riely GJ, Shaw AT. Targeting ALK: precision medicine takes on drug resistance. Cancer Discov 2017;7:137–55.
11. Santarpia M, Altavilla G, Rosell R. Alectinib: a selective, next-generation ALK inhibitor for treatment of ALK-rearranged non-small-cell lung cancer. Expert Rev Respir Med 2015;9:255–68.
12. Zou HY, Friboulet L, Kodack DP, Engstrom LD, Li Q, West M, et al. PF-06463922, an ALK/ROS1 inhibitor, overcomes resistance to first and second generation ALK inhibitors in preclinical models. Cancer Cell 2015;28:70–81.

13. Eisenhauer EA, Therasse P, Bogaerts J, Schwartz LH, Sargent D, Ford R, et al. New response evaluation criteria in solid tumours: revised RECIST guideline (version 1.1). Eur J Cancer 2009;45:228–47.
14. Favero F, Joshi T, Marquard AM, Birkbak NJ, Krzystanek M, Li Q, et al. Sequenza: allele-specific copy number and mutation profiles from tumor sequencing data. Ann Oncol 2015;26:64–70.
15. Newman AM, Bratman SV, Stehr H, Lee LJ, Liu CL, Diehn M, et al. FACTERA: a practical method for the discovery of genomic rearrangements at breakpoint resolution. Bioinformatics 2014;30:3390–3.
16. Woo CG, Seo S, Kim SW, Jang SJ, Park KS, Song JY, et al. Differential protein stability and clinical responses of EML4-ALK fusion variants to various ALK inhibitors in advanced ALK-rearranged non-small cell lung cancer. Ann Oncol 2017;28:791–7.
17. Drilon A, Rekhtman N, Arcila M, Wang L, Ni A, Albano M, et al. Cabozantinib in patients with advanced RET-rearranged non-small-cell lung cancer: an open-label, single-centre, phase 2, single-arm trial. Lancet Oncol 2016;17:1653–60.
18. Wiesner T, He J, Yelensky R, Esteve-Puig R, Botton T, Yeh I, et al. Kinase fusions are frequent in Spitz tumours and spitzoid melanomas. Nat Commun 2014;5:3116.
19. Fang DD, Zhang B, Gu Q, Lira M, Xu Q, Sun H, et al. HIP1-ALK, a novel ALK fusion variant that responds to crizotinib. J Thorac Oncol 2014;9:285–94.
20. Hong M, Kim RN, Song JY, Choi SJ, Oh E, Lira ME, et al. HIP1-ALK, a novel fusion protein identified in lung adenocarcinoma. J Thorac Oncol 2014;9:419–22.
21. Jiang J, Wu X, Tong X, Wei W, Chen A, Wang X, et al. GCC2-ALK as a targetable fusion in lung adenocarcinoma and its enduring clinical responses to ALK inhibitors. Lung Cancer 2018;115:5–11.
22. Vendrell JA, Taviaux S, Beganton B, Godreuil S, Audran P, Grand D, et al. Detection of known and novel ALK fusion transcripts in lung cancer patients using next-generation sequencing approaches. Sci Rep 2017;7:12510.
23. Kron A, Alidousty C, Scheffler M, Merkelbach-Bruse S, Seidel D, Riedel R, et al. Impact of TP53 mutation status on systemic treatment outcome in ALK-rearranged non-small-cell lung cancer. Ann Oncol 2018;29:2068–75.
24. Friboulet L, Li N, Katayama R, Lee CC, Gainor JF, Crystal AS, et al. The ALK inhibitor ceritinib overcomes crizotinib resistance in non-small cell lung cancer. Cancer Discov 2014;4:662–73.
25. Botting GM, Rastogi I, Chhabra G, Nlend M, Puri N. Mechanism of resistance and novel targets mediating resistance to EGFR and c-Met tyrosine kinase inhibitors in non-small cell lung cancer. PLoS One 2015;10:e0136155.
26. Kang J, Chen HJ, Zhang XC, Su J, Zhou Q, Tu HY, et al. Heterogeneous responses and resistant mechanisms to crizotinib in ALK-positive advanced non-small cell lung cancer. Thorac Cancer 2018;9:1093–103.
27. Wang WX, Xu CW, Chen YP, Liu W, Zhong LH, Chen FF, et al. TP53 mutations predict for poor survival in ALK rearrangement lung adenocarcinoma patients treated with crizotinib. J Thorac Dis 2018;10:2991–8.
28. Joerger AC, Fersht AR. Structural biology of the tumor suppressor p53 and cancer-associated mutants. Adv Cancer Res 2007;97:1–23.
29. Li Y, Zhang T, Zhang J, Li W, Yuan P, Xing P, et al. Response to crizotinib in advanced ALK-rearranged non-small cell lung cancers with different ALK-fusion variants. Lung Cancer 2018;118:128–33.
30. Yoshida T, Oya Y, Tanaka K, Shimizu J, Horio Y, Kuroda H, et al. Differential crizotinib response duration among ALK fusion variants in ALK-positive non-small-cell lung cancer. J Clin Oncol 2016;34:3383–9.